Redox Biology 63 (2023) 102749

Contents lists available at ScienceDirect

Redox Biology

journal homepage: www.elsevier.com/locate/redox

Glycerol as a precursor for hepatic *de novo* glutathione synthesis in human liver

Eunsook S. Jin [a,b], Craig R. Malloy [a,b,c,e], Gaurav Sharma [d,e], Erin Finn [f,g], Kelly N.Z. Fuller [f,g], Yesenia Garcia Reyes [f,g], Mark A. Lovell [g,h], Sarkis C. Derderian [g,i], Jonathan A. Schoen [g,i], Thomas H. Inge [g,i,j], Melanie G. Cree [f,g,*]

[a] *Advanced Imaging Research Center, University of Texas Southwestern Medical Center, Dallas, TX, 75390, USA*
[b] *Department of Internal Medicine, University of Texas Southwestern Medical Center, Dallas, TX, 75390, USA*
[c] *Department of Radiology, University of Texas Southwestern Medical Center, Dallas, TX, 75390, USA*
[d] *Department of Cardiovascular & Thoracic Surgery, University of Texas Southwestern Medical Center, Dallas, TX, 75390, USA*
[e] *VA North Texas Health Care System, Dallas, TX, 75216, USA*
[f] *Department of Pediatrics, University of Colorado School of Medicine Anschutz Medical Campus, Aurora, CO, 80045, USA*
[g] *Children's Hospital of Colorado, Aurora, CO, 80045, USA*
[h] *Department of Pathology, University of Colorado School of Medicine Anschutz Medical Campus, Aurora, CO, 80045, USA*
[i] *Department of Surgery, University of Colorado School of Medicine Anschutz Medical Campus, Aurora, CO, 80045, USA*
[j] *Ann and Robert Lurie Children's Hospital of Chicago, USA*

A R T I C L E I N F O

Keywords:
Glycerol
Glycine
Glutamate
Cysteine
Liver
Glutathione
Stable isotope
NMR

A B S T R A C T

Background: Glycerol is a substrate for gluconeogenesis and fatty acid esterification in the liver, processes which are upregulated in obesity and may contribute to excess fat accumulation. Glycine and glutamate, in addition to cysteine, are components of glutathione, the major antioxidant in the liver. In principle, glycerol could be incorporated into glutathione via the TCA cycle or 3-phosphoglycerate, but it is unknown whether glycerol contributes to hepatic *de novo* glutathione biosynthesis.

Methods: Glycerol metabolism to hepatic metabolic products including glutathione was examined in the liver from adolescents undergoing bariatric surgery. Participants received oral [U–$^{13}C_3$]glycerol (50 mg/kg) prior to surgery and liver tissue (0.2–0.7g) was obtained during surgery. Glutathione, amino acids, and other water-soluble metabolites were extracted from the liver tissue and isotopomers were quantified with nuclear magnetic resonance spectroscopy.

Results: Data were collected from 8 participants (2 male, 6 female; age 17.1 years [range 14–19]; BMI 47.4 kg/m^2 [range 41.3–63.3]). The concentrations of free glutamate, cysteine, and glycine were similar among participants, and so were the fractions of ^{13}C-labeled glutamate and glycine derived from [U–$^{13}C_3$]glycerol. The signals from all component amino acids of glutathione - glutamate, cysteine and glycine - were strong and analyzed to obtain the relative concentrations of the antioxidant in the liver. The signals from glutathione containing [$^{13}C_2$]glycine or [$^{13}C_2$]glutamate derived from the [U–$^{13}C_3$]glycerol drink were readily detected, and ^{13}C-labelling patterns in the moieties were consistent with the patterns in corresponding free amino acids from the *de novo* glutathione synthesis pathway. The newly synthesized glutathione with [U–$^{13}C_3$]glycerol trended to be lower in obese adolescents with liver pathology.

Conclusions: This is the first report of glycerol incorporation into glutathione through glycine or glutamate metabolism in human liver. This could represent a compensatory mechanism to increase glutathione in the setting of excess glycerol delivery to the liver.

1. Introduction

Non-alcoholic fatty liver disease (NAFLD) is growing in prevalence,

* Corresponding author. 13123 E16th Avenue, Aurora, CO, 80045, USA.
E-mail address: Melanie.green@childrenscolorado.org (M.G. Cree).

https://doi.org/10.1016/j.redox.2023.102749
Received 18 April 2023; Received in revised form 10 May 2023; Accepted 14 May 2023
Available online 16 May 2023

Nomenclature

Ala	alanine
ALT	alanine transaminase
BMI	body mass index
Cys	cysteine
D	doublet
DHAP	dihydroxyacetone phosphate
DSS	4,4-dimethyl-4-silapentane-1-sulfonic acid
GA3P	glyceraldehyde 3-phosphate
GCL	glutamate cysteine ligase
Glu	glutamate
Gly	glycine
GPx	glutathione peroxidases
GR	glutathione reductase
GS	glutathione synthetase
GSH	glutathione (reduced form)
GSSG	glutathione disulfide (oxidized form)
α-kG	α-ketoglutarate
Lac	lactate
MRI	magnetic resonance imaging
NAC	N-acetylcysteine
NAFLD	non-alcoholic fatty liver disease
NASH	non-alcoholic steatohepatitis
NMR	nuclear magnetic resonance
OAA	oxaloacetate
PC	pyruvate carboxylase
PDH	pyruvate dehydrogenase
3 PG	3-phosphoglycerate
PHGDH	phosphoglycerate dehydrogenase
PSAT	phosphoserine aminotransferase
PSPH	phosphoserine phosphatase
S	singlet
SHMT	serine hydromethyl transferase
TCA	tricarboxylic acid

related to increasing rates of obesity, with very concerning rates in adolescents [1,2]. Fatty liver disease is projected to be the leading cause of hepatic transplantation [3]. Of particular interest is what determines progression of simple steatosis to non-alcoholic steatohepatitis (NASH) as not all adolescents with fatty liver progress to NASH or fibrosis [4]. This process has been tied to increased inflammation in the liver, in particular reactive oxygen species and oxidative stress [5]. A critical part of the development of new pharmaceuticals is gaining a full understanding of hepatocyte substrate metabolism which may be involved in the development of NASH.

Glutathione is the major antioxidant in the body protecting cells from reactive oxygen species and free radicals [6–8]. It is a tripeptide composed of glutamate (Glu), cysteine (Cys), and glycine (Gly). Glutathione exists in two forms, the reduced form (GSH) and the oxidized form (GSSG, glutathione disulfide). The thiol group (-SH) of the cysteine moiety in GSH provides a reducing equivalent, and the oxidation of GSH leads to GSSG that has a disulfide bond between two molecules of GSH (Fig. 1A). GSH is dominant *in vivo*, but the fraction of GSSG increases under oxidative stress and other pathophysiological conditions [9–11]. Glutathione is maintained at a high concentration in most cells, particularly in hepatocytes [7,8,10,12], but its concentration decreases with chronic degenerative diseases or aging [13].

The liver is the main source of glutathione in the body, and the antioxidant synthesized in the liver is exported to other organs through blood and bile [14]. Among the constituent amino acids in glutathione, the availability of cysteine is the rate-limiting factor in *de novo* glutathione synthesis, catalyzed by glutamate-cysteine ligase [15]. The supply of cysteine or its precursors stimulates glutathione synthesis [8]. N-acetylcysteine (NAC), a well-known precursor to cysteine, is used for the treatment of acetaminophen poisoning by replenishing glutathione in the liver and for the treatment of other diseases associated with oxygen radicals [16–18]. Under some circumstances such as diabetes or protein malnutrition, glycine may limit glutathione synthesis [19–21]. Low circulating glycine was reported to limit glutathione biosynthesis in fatty liver [22,23]. The administration of glycine alone, combination with NAC, or serine as a precursor also increases glutathione [24–28]. Glutamate, however, has received less attention related to its regulatory role in glutathione biosynthesis, presumably due to its abundance in most cells.

The liver receives ample nutrients through the portal vein including glycerol derived from lipolysis of triglycerides in visceral fat and from the diet. Glycerol is utilized for gluconeogenesis and fatty acid esterification producing glucose and triglycerides, respectively. Since glycerol may enter glycolytic pathways, it can be metabolized to glycine through 3-phosphoglycerate. Glycerol may also be metabolized to pyruvate and, after entry into the TCA cycle, undergo metabolism to glutamate [29]. Thus, while it is conceivable that glycerol contributes to glutathione through glycine or glutamate, glycerol incorporation into glutathione has not been reported previously in human liver. The purposes of this study are to determine the metabolic pathways involved in glycerol metabolism in the human liver and to specifically investigate the contribution of glycerol to *de novo* glutathione synthesis. We recruited adolescents who were undergoing bariatric surgery and administered oral [U–$^{13}C_3$]glycerol prior to surgery. A liver biopsy was performed during surgery and the tissue extracts were analyzed using nuclear magnetic resonance (NMR) spectroscopy to determine glycerol incorporation into glutathione and relevant metabolic processes.

2. Materials and methods

2.1. Research design

Participants: Youth aged 13–20 years old with body mass index (BMI) 41.3–63.3 kg/m^2 (n = 8) were recruited from the bariatric surgery clinic at Children's Hospital Colorado (Colorado Multiple IRB 18–0479, NCT03587727). Exclusion criteria included a history of type 2 diabetes, viral hepatitis, mitochondrial disease, the use of medications known to alter insulin resistance including atypical antipsychotics, immunosuppressants, HIV medications, PPAR-γ or PPAR-α, and metformin, MRI exclusion criteria including largest circumference >200 cm and implanted metal, pregnancy, alcohol abuse, hemoglobin <10 mg/dL, and psychiatric or developmental concerns limiting informed assent and consent. The study was approved by the Colorado Institutional Review Board. All participants <18 years old provided written assent with parental consent and participants ≥18 years old provided written consent prior to enrollment and performance of any research.

Study Design: Participants underwent fasting metabolic assessments with labs and anthropomorphic measurements. Fasting laboratory values were drawn within 7 days prior to laparoscopic vertical sleeve gastrectomy. On the day of surgery, oral [U–$^{13}C_3$]glycerol (50 mg/kg body weight; Cambridge Isotope Laboratories, Inc. Tewksbury, MA USA) was consumed after overnight fast and 2 h prior to scheduled procedure start. Liver core and wedge biopsies were obtained for clinical and NMR analyses. Due to variation in operative schedules, biopsies occurred between 1.5 and 5.5 h after glycerol consumption (Fig. S1 and Table 1). Liver tissue was preserved immediately following biopsy by flash freezing in liquid nitrogen and stored at −80 °C prior to sample preparation for NMR spectroscopy.

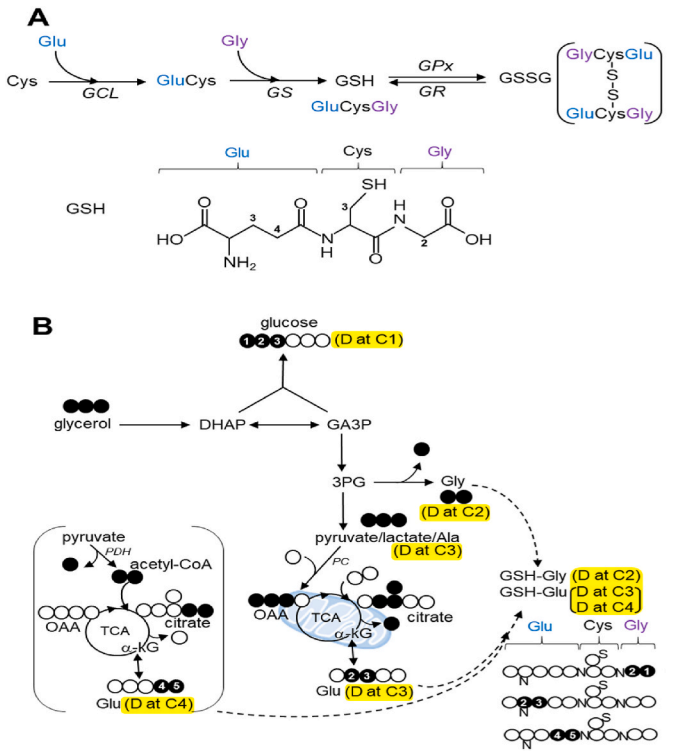

Fig. 1. Glutathione biosynthesis and NMR detection for [U–$^{13}C_3$] glycerol incorporation to glutathione (**A**) In glutathione biosynthesis, γ-glutamylcysteine (GluCys) is formed from glutamate and cysteine via glutamate cysteine ligase (GCL) followed by the reaction between the dipeptide and glycine via glutathione synthetase (GS). The oxidation of reduced glutathione (GSH) to glutathione disulfide (GSSG) is catalyzed by glutathione peroxidase (GPx) while GSH regeneration from GSSG is catalyzed by glutathione reductase (GR). The numbers in glutathione chemical structure indicate the carbon positions of component amino acids selected for NMR analysis. (**B**) A simplified schematic shows glycerol metabolism in liver. Glycerol is converted to dihydroxyacetone phosphate (DHAP) or glyceraldehyde 3-phosphate (GA3P). The condensation of the two trioses leads to glucose and gluconeogenesis from [U–$^{13}C_3$]glycerol produces triple-labeled glucose ([$^{13}C_3$]glucose). GA3P may enter glycolytic pathway producing pyruvate that is in exchange with lactate or alanine (Ala). [U–$^{13}C_3$]glycerol metabolism through the glycolysis leads to triple-labeled ([$^{13}C_3$]) lactate or alanine. Pyruvate enters the TCA cycle through pyruvate carboxylase (PC) or dehydrogenase (PDH). [U–$^{13}C_3$]pyruvate becomes [1,2,3–$^{13}C_3$]oxaloacetate (OAA) through PC, and the condensation between [1,2,3–$^{13}C_3$]oxaloacetate and acetyl-CoA produces [2,3,6–$^{13}C_3$]citrate and then [2,3–$^{13}C_2$]α-ketoglutarate (α-kG) through the TCA cycle. Since α-ketoglutarate is in exchange with glutamate, the detection of [2,3–$^{13}C_2$]glutamate is evidence of PC activity. In contrast, PDH produces [1,2–$^{13}C_2$]acetyl-CoA from [U–$^{13}C_3$] pyruvate, and the reaction between [1,2–$^{13}C_2$]acetyl-CoA and oxaloacetate leads to [4,5–$^{13}C_2$]citrate, [4,5–$^{13}C_2$]α-ketoglutarate and consequently [4,5–$^{13}C_2$]glutamate. Thus, [U–$^{13}C_3$]glycerol incorporation to glutathione through glutamate produces [2,3–$^{13}C_2$]glutamate moiety or [4,5–$^{13}C_2$]glutamate moiety. Glycerol can be converted to glycine through 3-phosphoglycerate (3 PG), and [U–$^{13}C_3$]glycerol incorporation to glutathione through glycine produces glutathione-[$^{13}C_2$]glycine. Highlights with yellow indicate doublet (D) signals in ^{13}C NMR spectra of metabolic products derived from [U–$^{13}C_3$] glycerol. open circle, ^{12}C; black circle, ^{13}C. (For interpretation of the references to colour in this figure legend, the reader is referred to the Web version of this article.)

Liver biopsies were evaluated by author MAL in the clinical pathology service at Children's Hospital Colorado using standard liver pathology techniques [30]. The liver biopsy was preserved in 10% neutral buffered formalin for fixation, embedded in paraffin, and sectioned on a microtome at 4 μm followed by staining with routinely performed hematoxylin and eosin, trichrome, and periodic acid-Schiff with and without diastase.

2.2. Sample preparation and NMR spectroscopy

Metabolites were extracted from liver tissues using a method reported previously with modifications [31]. Frozen liver tissue (0.2–0.7 g) was powdered using a mortar and pestle chilled with liquid nitrogen, and ground tissue was transferred into a 15-mL conical tube containing a mixture of acetonitrile-isopropanol-water (3:3:2; 7 mL) on ice, vortexed for 1 min, and centrifuged at 25,000 g and 4 °C for 10 min. The supernatant was transferred to a 50-mL conical tube, and the remaining pellet was treated with the additional mixture of acetonitrile-isopropanol-water (5 mL). The pellet was disrupted with a spatula, vortexed for 1 min and centrifuged, and the supernatant was transferred to the same 50-mL tube. The extraction was repeated one more time by adding the mixture of solvents (3 mL) to the pellet. Combined supernatant was centrifuged at 25,000 g and 4 °C for 10 min and it was transferred to a 20-mL glass vial to dry under vacuum. Dichloromethane (1 mL x 3) was slowly added to dried extracts to dissolve lipids, and dichloromethane solution was transferred to a new 15-mL conical tube. After centrifuging, the dichloromethane solution was discarded, and the residue was dissolved with the mixture of acetonitrile-isopropanol-water (100 μL x 3) to combine with the original extracts in the 20-mL glass vial. After drying under vacuum, the extracts were dissolved in heavy water (^2H_2O, 200 μL) containing 4,4-dimethyl-4-silapentane-1-sulfonic acid (DSS; 5 mM; NMR reference), centrifuged at 20,000 g for 5 min and the supernatant was transferred to a 3-mm NMR tube.

NMR spectra were collected using a 14.1 T Bruker Avance III HD equipped with a 5-mm cryoprobe (Bruker, MA, USA) with the observe coil tuned to ^{13}C (150 MHz). Proton-decoupled ^{13}C NMR was acquired using Bruker standard zgpg30 sequence (a 30° pulse, a 36k-Hz sweep width, and a 2-s acquisition time with 1.5-s interpulse delay) at 25 °C. Proton decoupling was performed using a standard WALTZ-16 pulse sequence. Spectra were averaged with 8000–20,000 scans and a line broadening of 0.5 Hz was applied prior to Fourier transformation. Spectra were analyzed using ACD/Labs NMR spectral analysis program (Advanced Chemistry Development, Inc., Toronto, Canada).

2.3. NMR analysis of metabolites

In the liver, [U–$^{13}C_3$]glycerol is phosphorylated by glycerol kinase and can be further converted to another triose such as dihydroxyacetone phosphate (DHAP) or glyceraldehyde 3-phosphate (GA3P). Since the condensation of these two trioses leads to glucose, the appearance of triple-labeled (i.e., [1,2,3–$^{13}C_3$] or [4,5,6–$^{13}C_3$]) glucose is evidence of gluconeogenesis from [U–$^{13}C_3$]glycerol (Fig. 1B). In this study, [1,2,3–$^{13}C_3$]glucose was quantified using the peak areas of doublets (D12) at α-glucose carbon 1 (C1; 93.2 ppm; Fig. 2A) and β-glucose C1 (97.0 ppm). Instead of entering gluconeogenesis, [U–$^{13}C_3$]GA3P may experience the terminal steps of glycolysis to produce pyruvate that is in exchange with lactate or alanine (Ala). Thus, the appearance of [U–$^{13}C_3$] lactate or [U–$^{13}C_3$]alanine is evidence of [U–$^{13}C_3$]glycerol metabolism through glycolysis. These products were detected using the doublet (D23) at lactate C3 (21.2 ppm) or alanine C3 (17.3 ppm), respectively. 3-phosphoglycerate (3 PG) is an intermediate of glycolysis and it can be metabolized to serine through the multiple enzymatic activities of phosphoglycerate dehydrogenase (PHGDH), phosphoserine aminotransferase (PSAT), and phosphoserine phosphatase (PSPH), and then glycine after decarboxylation by serine hydromethyl transferase (SHMT). [U–$^{13}C_3$]glycerol metabolism to glycine was detected by the doublet at glycine C2 (42.5 ppm) in ^{13}C NMR, a signal from [U–$^{13}C_2$] glycine.

Pyruvate enters the TCA cycle through pyruvate dehydrogenase (PDH) or pyruvate carboxylase (PC). The entry of [U–$^{13}C_3$]pyruvate through PDH produces [1,2–$^{13}C_2$]acetyl-CoA after decarboxylation, and the condensation between [1,2–$^{13}C_2$]acetyl-CoA and oxaloacetate (OAA) generates [4,5–$^{13}C_2$]citrate and then [4,5–$^{13}C_2$]α-ketoglutarate

Table 1
Clinical characteristics of participants.

Patient	#1	#2	#3	#4	#5	#6	#7	#8
Characteristic								
Age (year)	14.8	17.8	18.3	16.2	16.4	19.0	15.0	18.9
Sex (Female/Male)	F	F	F	F	M	F	M	F
Race (Black/White/Other)	W	W	Other	W	Multiple	W	W	W
Ethnicity (Hispanic/Not Hispanic)	H	H	NH	H	H	NH	H	H
Body weight (kg)	136.4	138.8	118.0	129.2	154.7	168.3	125.8	106.3
Body mass index (kg/m^2)	43.5	49.8	42.5	52.1	44.5	63.3	41.6	41.3
Plasma								
Hemoglobin A1c (%)	6.1	5.6	5.0	5.8	5.5	4.9	5.4	5.4
Triglycerides (<90 mg/dL)	223	121	89	106	66	150	128	97
ALT (11–26 U/L)	23	21	32	71	46	14	116	29
AST (15–40 U/L)	26	23	25	47	35	23	51	31
Liver								
Steatosis grade	1	1	0	3	0	0	3	3
Steatosis location	zone 1	zone 2	ND[a]	azonal	ND	azonal	zone 3	panacinar
Lobular inflammation	1	0	0	1	0	0	1	0
Liver cell injury (ballooning)	0	2	0	1	0	0	0	0
Fibrosis stage	1C	1A	0	1A	0	1C	0	0
Liver biopsy								
Time after ^{13}C-glycerol (hr)	5.5	4.8	3.5	2.6	3.6	4.5	1.5	3.5
Tissue mass for NMR (g)	0.35	0.75	0.33	0.29	0.65	0.31	0.22	0.22

[a] ND, not detected.

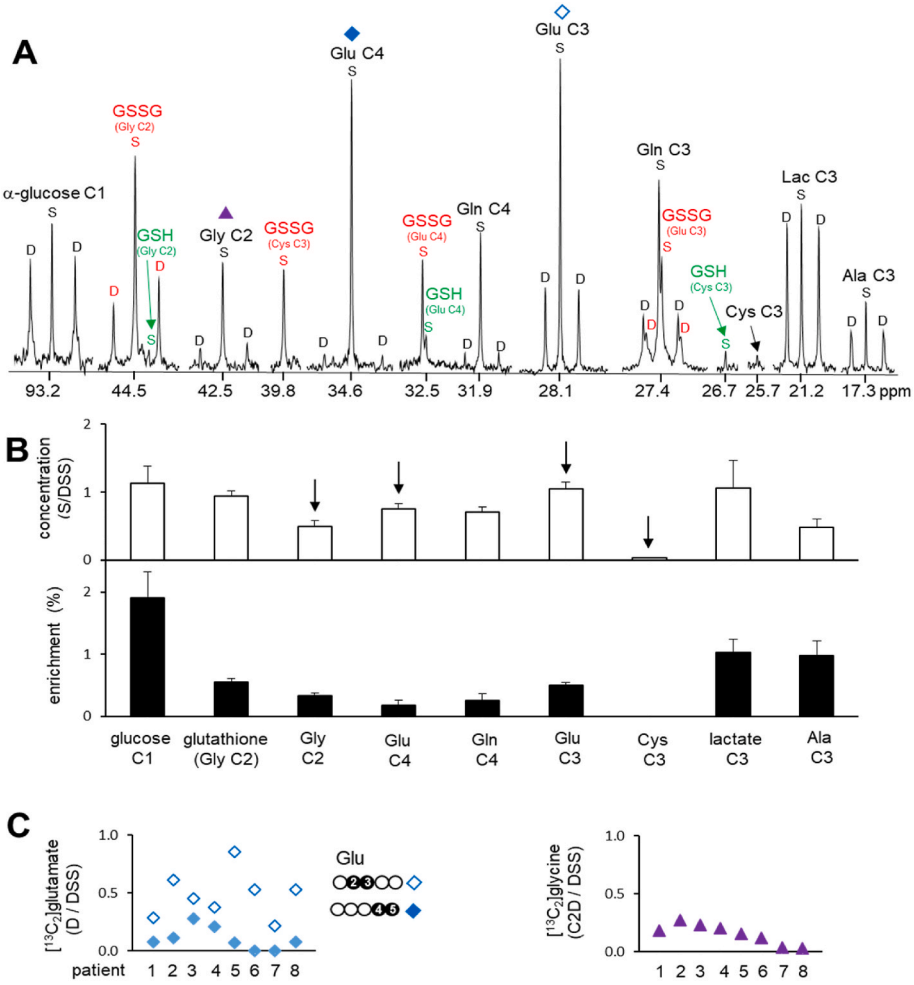

Fig. 2. NMR analysis of metabolites in liver extracts (**A**) In ^{13}C NMR, a singlet (S) reflects the pool size of a metabolite with natural ^{13}C abundance and a double (D) is the signal from ^{13}C–^{13}C spin-spin coupling with two adjacent carbons originated from [U–$^{13}C_3$]glycerol. A doublet at glucose C1 is from [1,2,3–$^{13}C_3$]glucose demonstrating gluconeogenesis from [U–$^{13}C_3$]glycerol while a doublet at lactate C3 is from [U–$^{13}C_3$]lactate demonstrating the glycerol metabolism through glycolytic pathway. Doublet signals from other metabolites also inform [U–$^{13}C_3$] glycerol metabolism to glycine, glutamate, glutamine, glutathione and so on. (**B**) Graphs show relative concentrations of metabolites and their enrichments based on NMR analysis. Arrows indicate free glycine, glutamate and cysteine. Cysteine was not enriched by ^{13}C and its concentration was low. Data are average ± SE (n = 8). (**C**) Graphs show relative concentrations of [2,3–$^{13}C_2$]glutamate, [4,5–$^{13}C_2$]glutamate and [1,2–$^{13}C_2$]glycine based on doublet signals from the amino acids.

(αKG) through the TCA cycle. Since α-ketoglutarate is in exchange with glutamate, glycerol metabolism through PDH produces [4,5–$^{13}C_2$] glutamate that can be detected by a doublet (D45, J_{CC} ~ 52 Hz) at glutamate C4 (34.6 ppm) in ^{13}C NMR (Fig. 2A). The entry of [U–$^{13}C_3$] pyruvate through PC produces [1,2,3–$^{13}C_3$]oxaloacetate after carboxylation, and the reaction between [1,2,3–$^{13}C_3$]oxaloacetate and acetyl-

CoA produces [2,3,6–$^{13}C_3$]citrate. The citrate becomes [2,3–$^{13}C_2$]α-ketoglutarate through the TCA cycle and then [2,3–$^{13}C_2$]glutamate that can be quantified using a doublet (D23, J_{CC} ~ 34 Hz) at glutamate C3 (28.1 ppm; Fig. 2A).

The relative concentration of a metabolite was calculated based on the peak area of a singlet (S) from each metabolite because the singlet represents natural ^{13}C abundance. The level of a ^{13}C-labeled metabolite derived from [U–$^{13}C_3$]glycerol was measured using a doublet (D), a signal from ^{13}C–^{13}C spin-spin coupling (Fig. 2A). The peak area of a singlet or a doublet was normalized by the peak area of DSS, the NMR reference.

2.4. NMR analysis of glutathione

Signals from GSH and GSSG were resolved in ^{13}C NMR spectra (Figs. 2A and 3A). Among many carbons in glutathione, signals from glycine moiety C2, cysteine moiety C3, and glutamate moiety C3 and C4 were selected for analysis because these signals were stronger and better resolved compared to signals from other carbons. Chemical shifts and NMR signals from the selected carbons in GSH and GSSG are as follow:

Glutamate C3 in GSH and GSSG at 27.4 ppm: S ([3–$^{13}C_1$]Glu) and D23 ([2,3–$^{13}C_2$]Glu).

Glutamate C4 in GSH and GSSG at 32.5 ppm: S ([4–$^{13}C_1$]Glu) and D45 ([4,5–$^{13}C_2$]Glu).

Cysteine C3 in GSH at 26.7 ppm and GSSG at 39.8 ppm: S ([3–$^{13}C_1$]Cys).

Glycine C2 in GSH and GSSG at 44.5 ppm: S ([2–$^{13}C_1$]Gly) and D ([U–$^{13}C_2$]Gly).

A singlet (S) reflects the pool size of glutathione with natural ^{13}C abundance and a doublet (D) is evidence of [U–$^{13}C_3$]glycerol metabolism to glutathione. Doublets were detected in glutamate and glycine moieties, but not in the cysteine moiety.

2.5. Statistical analysis

NMR Comparisons between two groups were made using a Mann Whitney *U* test for non-parametric data and ANOVA was used for analysis of greater than 2 groups, where $p < 0.05$ was considered significant. Data are expressed as mean ± standard error.

3. Theory

As previously described, the ^{13}C label from an oral load of [U–$^{13}C_3$]glycerol can be traced to specific locations within a metabolite, as detected by isotopomer NMR analysis. Label locations and signal abundance can be used to measure hepatic relative contributions of the TCA cycle, the pentose phosphate pathway and indirect metabolism, in both the glucose and triglyceride products that are released from the

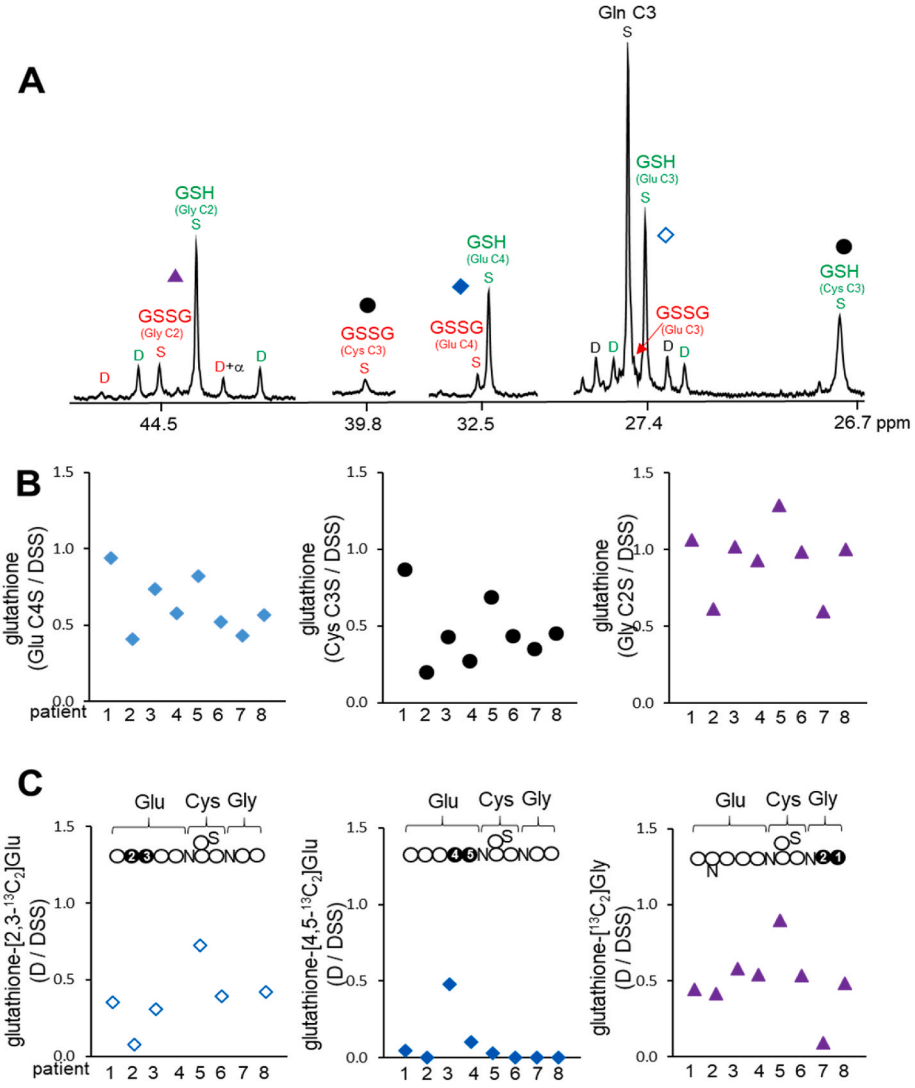

Fig. 3. Quantitation of glutathione and newly synthesized glutathione with [U–$^{13}C_3$] glycerol
(**A**) ^{13}C NMR of liver extracts shows signals from component amino acids in glutathione. Singlet signals represent the pool size of glutathione and doublets represent [U–$^{13}C_3$]glycerol incorporation to glutathione. (**B**) Graphs show relative glutathione contents (sum of GSH and GSSG) based on singlet signals from glutamate moiety C4, cysteine moiety C3 and glycine moiety C2 in ^{13}C NMR spectra. (**C**) Graphs show the relative level of glutathione containing [2,3–$^{13}C_2$] glutamate, [4,5–$^{13}C_2$]glutamate or [U–$^{13}C_2$]glycine. Newly synthesized glutathione with [U–$^{13}C_3$]glycerol should be cautiously compared among participants due to varied timing for a liver biopsy. The low level of newly synthesized glutathione in patient #7, for example, could be in part due to the short duration from [U–$^{13}C_3$]glycerol administration to liver biopsy (1.5 h).

liver [29]. In this study, we performed this isotopomer NMR analysis on liver tissue, rather than blood, and assessed for the location of the tracer in a broader range of metabolites, to better understand intrahepatic energy metabolism. By performing the analysis in the liver tissue, the hypothesis was that we would be able to find the ^{13}C label in a broader range of metabolites where either the enrichment was too low or there is not direct secretion to the blood stream.

4. Results

4.1. Participant characteristics

Clinical characteristics of participants are noted in Table 1. The average age of participants was 17.0 years with a range 14.8–19.0 years. Participants were predominantly female (75%) and identified as Hispanic (75%). Average BMI was 47.4 kg/m^2 with a range 41.3–63.3 kg/m^2. By design, no participants had diabetes (Hemoglobin A1c > 6.5%) and two had prediabetes (defined as hemoglobin A1c 5.7–6.4%). Five participants had elevations in ALT, two were >2x upper limit normal. Five of eight had hepatic steatosis, three had inflammation consistent with NASH, and four had some degree of fibrosis.

4.2. Assessment of metabolites and glycerol metabolism in the liver

Gluconeogenesis from [U–$^{13}C_3$]glycerol was evidenced by doublet (D12) signals at α-glucose C1 (93.2 ppm) and β-glucose C1 (97.0 ppm). [U–$^{13}C_3$]glycerol incorporation into glycolytic pathway was also evidenced by doublet (D23) signals at lactate C3 (21.2 ppm) and alanine C3 (17.3 ppm; Fig. 2A). The amplitude of the doublet relative to the natural abundance singlet in glucose, alanine and lactate indicates that ~1–3% of the metabolite pools were enriched by [U–$^{13}C_3$]glycerol (Fig. 2B). A doublet at glycine C2 (42.5 ppm), the signal from [U–$^{13}C_2$]glycine, was also detected demonstrating [U–$^{13}C_3$]glycerol metabolism to glycine. A small singlet only, without a doublet, was detectable at cysteine C3 (25.7 ppm). The relative concentrations and ^{13}C enrichments of these metabolites in the liver from each participant are listed in Table 2.

As noted, ^{13}C-labeling patterns in glutamate provide information about the path of pyruvate entry to the TCA cycle through PC or PDH. Both [2,3–$^{13}C_2$]glutamate (doublet at glutamate C3; 28.1 ppm) and [2,3–$^{13}C_2$]glutamine (doublet at glutamine C3; 27.4 ppm) were detected demonstrating [U–$^{13}C_3$]glycerol metabolism through PC. In addition, the presence of [4,5–$^{13}C_2$]glutamate (doublet at glutamate C4; 34.6 ppm) and [4,5–$^{13}C_2$]glutamine (doublet at glutamine C4; 31.9 ppm) demonstrated [U–$^{13}C_3$]glycerol metabolism through PDH. The signal from [2.3–$^{13}C_2$]glutamate was stronger than that from [4,5–$^{13}C_2$]glutamate in all participants demonstrating pyruvate entry to the TCA cycle mainly through PC rather than PDH.

Glutamate and glycine were abundant in the liver of all participants, but the concentration of cysteine was low (Fig. 2A–B). The levels of these free amino acids among participants were similar. The presence of ^{13}C-labeled glutamate and glycine showed active [U–$^{13}C_3$]glycerol metabolism to these amino acids in all participants. The levels of [$^{13}C_2$]glycine were not noticeably different among patients, but the levels of [$^{13}C_2$]glutamate varied (Fig. 2C).

4.3. Assessment of glutathione

The relative concentration and ^{13}C enrichment in hepatic glutathione were based on the signals from glycine moiety C2, cysteine moiety C3, glutamate moiety C3 and C4 (Fig. 3A). Chemical shifts for the carbons of component amino acids between GSH and GSSG were very close, except the cysteine moiety C3 (26.7 ppm in GSH; 39.8 ppm in GSSG). The different chemical shifts in the cysteine moiety were due to dissimilar chemical environments between a thiol (-SH) group in GSH and a disulfide bond (-S-S-) in GSSG. The relative concentration of total glutathione (GSH and GSSG) was measured using singlets from glycine moiety C2, cysteine moiety C3, and glutamate moiety C4. The results based on the signals from different component amino acids in glutathione were generally consistent in each patient (Fig. 3B). The concentrations of glutathione were high and comparable with common metabolites such as glucose, glutamate, and lactate (Fig. 2B), and they somewhat varied among patients (Fig. 3B and Table 3).

Table 2
Relative concentrations and^{13}C enrichments of metabolites.

Metabolite	Chemical shift	#1	#2	#3	#4	#5	#6	#7	#8
Glucose (α & β; C1)	92.9 & 97.0 ppm	2.67	1.82	0.87	0.87	0.77	0.77	0.65	0.59
Glucose enrichment (%)		0.23	0.80	1.03	1.99	2.97	3.03	3.50	1.72
Glycerol 3-phosphate (C1)	63.3 ppm	0.32	0.64	0.39	0.12	0.28	ND[a]	ND	0.08
G3P enrichment (%)		0.14	0.88	0.95	0.40	1.91	ND	ND	ND
Serine (C2)	57.4 ppm	0.19	0.16	0.09	0.01	0.04	0.09	ND	0.08
Serine enrichment (%)		0.21	0.12	0.24	ND	ND	ND	ND	ND
Glycine (C2)	42.6 ppm	0.85	0.79	0.56	0.45	0.50	0.32	0.19	0.30
Glycine enrichment (%)		0.24	0.38	0.45	0.50	0.34	0.40	0.21	0.11
Phosphoethanolamine (N)	41.8 ppm	0.18	0.20	0.16	0.08	0.19	0.20	0.09	0.47
Succinate (C2&C3)	35.0 ppm	0.44	1.14	0.51	0.24	0.41	0.16	0.15	0.34
Succinate enrichment (%)	0.07	0.17	0.16	0.24	0.30	ND	ND	0.15	
Glutamate (C4)	34.0 ppm	1.07	1.06	0.57	0.47	0.96	0.74	0.52	0.59
Glutamate enrichment (%)	0.08	0.11	0.53	0.49	0.09	ND	ND	0.15	
Glutamine (C4)	31.8 ppm	1.11	0.65	0.82	0.64	0.66	0.68	0.44	0.68
Glutamine enrichment (%)		0.10	0.21	0.86	0.51	0.14	0.14	ND	0.10
Glutamate (C3)	27.9 ppm	1.31	1.42	0.91	0.78	1.37	0.99	0.77	0.82
Glutamate enrichment (%)	0.24	0.48	0.54	0.53	0.69	0.59	0.32	0.58	
Cysteine (C3)	25.7 ppm	0.03	0.05	0.01	0.03	0.06	0.04	0.02	0.03
Lactate (C3)	21.0 ppm	1.81	3.48	1.28	0.66	0.65	0.09	0.08	0.45
Lactate enrichment (%)		0.23	0.75	0.87	0.90	2.12	1.72	0.97	0.65
Alanine C3	17.3 ppm	0.92	0.93	0.73	0.63	0.27	0.10	ND	0.25
Alanine enrichment (%)		0.28	0.69	0.95	1.10	1.86	2.02	ND	0.89

Common metabolites were analyzed using ^{13}C NMR of liver extracts. The relative concentration of a metabolite was measured using a singlet with natural ^{13}C abundance normalized by DSS, a NMR reference. Excess ^{13}C enrichment in each metabolite was calculated using a doublet by assuming a singlet from the metabolite as natural abundance (1.1%). Since the amount of tissue collected through a biopsy varied among participants, the concentrations of metabolites were calculated for 1 g. ^{13}C enrichments in metabolites cannot be directly compared among participants because the interval from [U–$^{13}C_3$]glycerol administration to a liver biopsy varied.
[a] ND, not detected.

Table 3
Relative concentrations and ^{13}C enrichments of glutathione.

moiety	Chemical shift	#1	#2	#3	#4	#5	#6	#7	#8
GSSG-Gly C2	44.5 ppm	0.23	0.44	0.97	0.55	1.20	0.74	0.52	0.86
enrichment (%)		0.45	0.82	0.63	0.60	0.78	0.60	0.17	0.58
GSH-Gly C2	44.4 ppm	0.84	0.18	0.04	0.38	0.09	0.25	0.08	0.17
enrichment (%)		0.47	0.56	0.60	0.70	0.57	0.60	ND[a]	0.55
Sum (Gly moiety C2)		1.07	0.62	1.01	0.93	1.29	0.99	0.60	1.03
GSSG-Cys C3	39.8 ppm	0.12	0.12	0.39	0.24	0.60	0.39	0.34	0.35
GSH-Cys C3	26.7 ppm	0.75	0.09	0.04	0.04	0.08	0.04	0.02	0.11
Sum (Cys moiety C3)	0.87	0.21	0.43	0.28	0.68	0.43	0.36	0.46	
GSSG-Glu C4	32.5 ppm	0.14	0.23	0.52	0.26	0.59	0.32	0.43	0.38
enrichment (%)		ND	ND	0.77	0.20	0.06	ND	ND	ND
GSH-Glu C4	32.5 ppm	0.80	0.18	0.22	0.32	0.24	0.20	ND	0.19
enrichment (%)	0.07	ND	0.59	0.20	ND	ND	ND	ND	
Sum (Glu moiety C4)	0.94	0.41	0.74	0.58	0.83	0.52	0.43	0.57	
GSSG-Glu C3[s]	27.4 ppm	0.06	0.06	0.75	–	0.83	0.47	–	0.42
enrichment (%)		ND	ND	0.45	–	0.96	0.92	–	1.09
GSH-Glu C3	27.4 ppm	0.87	0.15	0.07	–	0.07	0.30	ND	0.14
enrichment (%)		0.45	0.58	ND	–	ND	ND	ND	ND
Sum (Glu moiety C3)		0.93	0.21	0.82	–	0.90	0.77	–	0.56

The relative concentration of glutathione was based on singlet signals from the carbons of component amino acids, glycine (Gly), cysteine (Cys) and glutamate (Glu), normalized by the signal of DSS. Excess ^{13}C enrichment was calculated using a doublet from glycine moiety C2, glutamate moiety C3 and C4 in glutathione by assuming a singlet from the corresponding carbon as natural abundance. Since the amount of tissue collected through a biopsy varied among participants, the concentration of glutathione was calculated for 1 g. ^{13}C enrichments in glutathione cannot be directly compared among participants because the interval from [U–$^{13}C_3$]glycerol administration to a liver biopsy varied.

[a] ND, not detected; [s]Due to overlap with glutamine C3, the quantitation of glutamate moiety C3 could be not-precise.

4.4. Glutathione derived from [U–$^{13}C_3$]glycerol through glycine or glutamate

[U–$^{13}C_3$]glycerol incorporation into glutathione was demonstrated by the detection of [$^{13}C_2$]glycine and [$^{13}C_2$]glutamate moieties in glutathione (Fig. 3C and Table 3). Glutathione-[$^{13}C_2$]glycine was readily observed in all participants, but its concentrations were somewhat varied among them. Notably, patient # 7 had trivial ^{13}C-labeled glycine moiety, possibly due to the shortest interval (1.5 h) between the glycerol load and the biopsy (Table 1). As seen in free glutamate, the glutamate moiety in glutathione had ^{13}Cs at carbons 2 & 3 or carbons 4 & 5 depending on pyruvate entry to the TCA cycle. Glutathione-[2,3–$^{13}C_2$] glutamate was detectable in most participants, except two patients (#4 and #7) having unresolved signals due to overlap with glutamine C3. Glutathione-[4,5–$^{13}C_2$]glutamate was also detectable, but only in a few volunteers. Also, the doublet from glutathione-[2,3–$^{13}C_2$]glutamate was

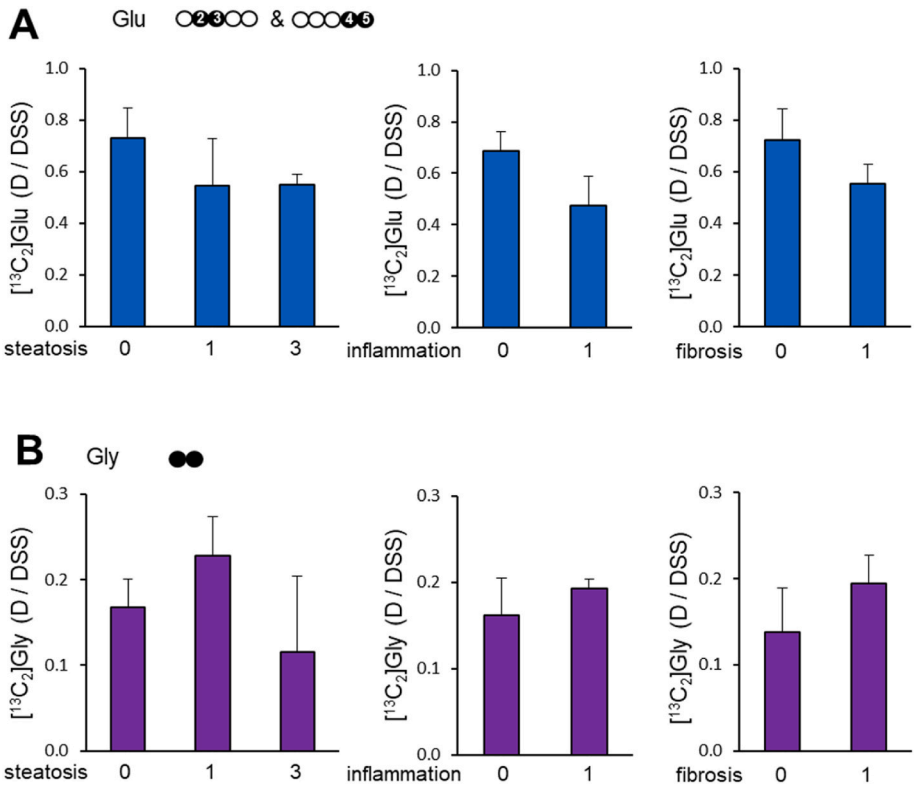

Fig. 4. Liver pathology vs. [U–$^{13}C_3$] glycerol metabolism to glutamate or glycine (**A**) [U–$^{13}C_3$] glycerol metabolism to glutamate was not significantly changed in the liver with steatosis, inflammation or fibrosis. [$^{13}C_2$]Glu at the x-axis is the sum of [2,3–$^{13}C_2$]glutamate and 4,5–$^{13}C_2$]glutamate. (**B**) According to the appearance of [U–$^{13}C_2$]glycine, [U–$^{13}C_3$]glycerol metabolism to glycine remained unchanged in the liver with steatosis, inflammation or fibrosis. The data from patient 7 was excluded due to a short duration from [U–$^{13}C_3$]glycerol administration to a liver biopsy.

generally larger than that from glutathione-[4,5–$^{13}C_2$]glutamate in each participant. The sum of [2,3–$^{13}C_2$]- and [4,5–$^{13}C_2$]glutamate moieties reflects glutathione synthesized from [U–$^{13}C_3$]glycerol regardless of pyruvate entry to the TCA cycle, and the sum was comparable among most participants, excepting patients #2 and #7 with minimal levels (Fig. 3C).

4.5. Liver pathology and [U–$^{13}C_3$]glycerol incorporation to glutathione

Among 8 participants, hepatic steatosis was detected in 5 patients, inflammation in 3 patients and fibrosis in 4 patients (Table 1). The levels of free ^{13}C-glutamate and ^{13}C-glycine were not different in these patients with different liver conditions (Fig. 4). Overall hepatic glutathione levels were not noticeably different depending on liver pathology, either (Fig. S2), but the levels of newly synthesized glutathione with [U–$^{13}C_3$]glycerol differed, $p = 0.05$. Glutathione synthesis through glutamate tended to decrease in the presence of steatosis or inflammation, and in the presence of fibrosis (Fig. 5A). In addition, glutathione synthesized through glycine tended to decrease with steatosis, inflammation or fibrosis without a statistical significance (Fig. 5B). Patient #7 was excluded in these analyses due to the exceptionally short duration (1.5 h) from [U–$^{13}C_3$]glycerol administration to the biopsy.

5. Discussion

We demonstrated metabolism of [U–$^{13}C_3$]glycerol to amino acids and incorporation into glutathione in the liver of adolescents undergoing bariatric surgery. Glycerol was metabolized to glycine or glutamate and both amino acids were further incorporated into *de novo* glutathione biosynthesis. To our knowledge, this is the first mammalian report of glycerol participation in hepatic glutathione synthesis. The levels of free glutamate, cysteine, glycine, ^{13}C-labeled glutamate, and ^{13}C-labeled glycine were generally similar among participants. Overall the levels of hepatic glutathione, glutathione-[$^{13}C_2$]glycine, and glutathione-[$^{13}C_2$]glutamate were high in most patients. However, there were obvious trends of lower newly synthesized glutathione with [U–$^{13}C_3$]glycerol in patients with liver pathology, and glutathione-[$^{13}C_2$]glutamate trended to be lower in the liver with fibrosis. It is difficult to draw definitive conclusions about some results because of varied timing for liver biopsy relative to glycerol administration, slightly different metabolic conditions for each patient, and intrahepatic heterogeneity among volunteers. Nevertheless, the current study clearly demonstrated that glycerol was a substrate for hepatic glutathione through glutamate or glycine metabolism, and glutathione synthesized with glycerol was reduced in obese youth with liver pathology.

Glycerol is well-known to serve as a substrate for gluconeogenesis and as the backbone for fatty acid esterification. This study proves a third role of glycerol in liver metabolism, incorporation into glutathione. The utilization of glycine or glutamate derived from [U–$^{13}C_3$]glycerol for glutathione biosynthesis was supported by consistent ^{13}C-labeling patterns between free amino acids and corresponding units in glutathione. The substrate incorporation to glutathione was not trivial because the amount of ^{13}C-labeled glutathione was comparable to those of ^{13}C-labeled common metabolites such as glucose and lactate, produced through gluconeogenesis and glycolytic pathway, respectively. In retrospect, glycerol metabolism to glutathione is not unexpected because metabolic pathways from glycerol to glycine or glutamate are established, and the incorporation of these amino acids into glutathione is also known. Glycerol from lipolysis of triglycerides may protect the liver from oxidative stress by contributing to glutathione synthesis. This new finding is interesting because the well-known roles of glycerol for glucose and triglyceride production are associated with poor glycemic

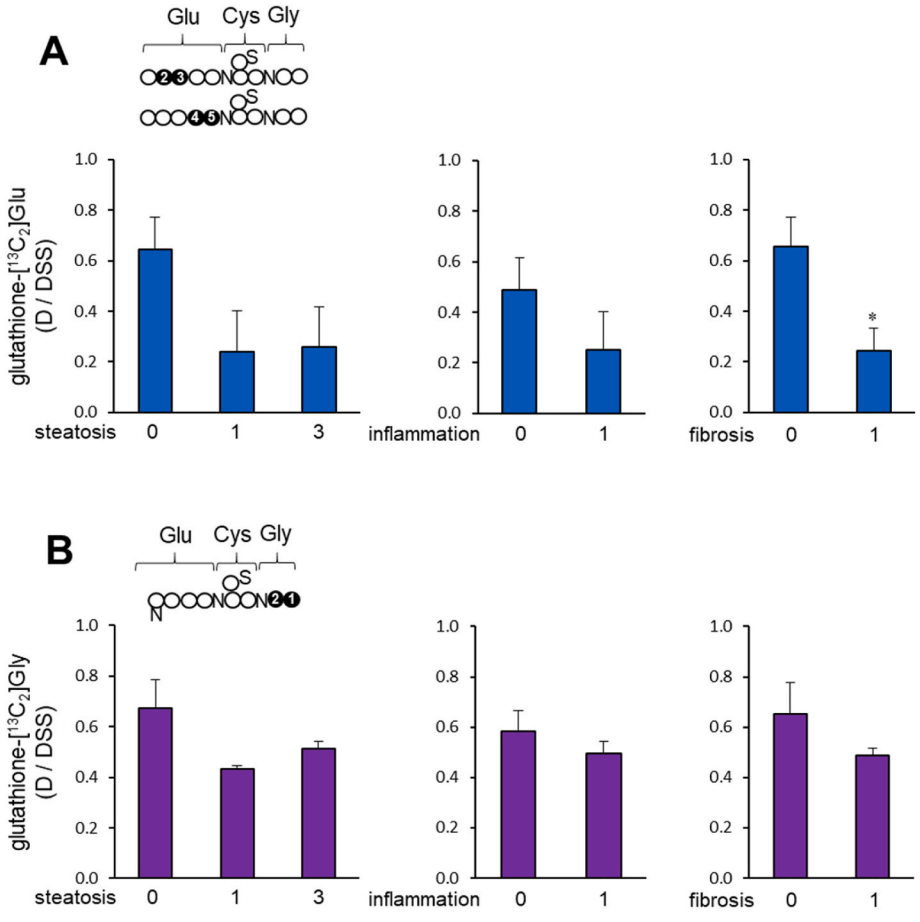

Fig. 5. Liver pathology vs. [U–$^{13}C_3$] glycerol incorporation to glutathione (**A**) The newly synthesized glutathione through glutamate after the administration of [U–$^{13}C_3$]glycerol significantly decreased in the liver with fibrosis, and tended to decrease in the presence of steatosis or inflammation without a statistical significance. Glutathione-[$^{13}C_2$]Glu at the x-axis is the sum of glutathione (GSH + GSSG) containing [2,3–$^{13}C_2$]glutamate and [4,5–$^{13}C_2$]glutamate. (**B**) Based on the amount of glutathione-[$^{13}C_2$]glycine, the newly synthesized glutathione through glycine tended to decrease in the liver with steatosis, inflammation or fibrosis without a statistical significance. The data from patient 7 was excluded due to a short duration from [U–$^{13}C_3$]glycerol administration to a liver biopsy.

control, excess lipid burden, and potentially oxidative stress [32,33]. Glycerol incorporation to glutathione must contribute to counteracting these adverse processes. Partitioning of glycerol released from lipolysis for the biosynthesis of glucose, triglycerides, or glutathione could play a role in the progression of fatty liver disease since it can be advantageous or disadvantageous for liver health depending on its metabolism. Asides component amino acids of glutathione and their precursors, contributions of other substrates to glutathione production are mostly unknown, but glucose was reported to produce the antioxidant in erythrocytes and pancreatic islets [34,35]. The earlier study with the islets specified PC activity needed for glutathione synthesis from glucose [34]. It was consistent with the current result about glycerol incorporation to glutathione through the series of processes including glycolytic pathway, PC, the TCA cycle and glutamate.

Though the two forms of glutathione (GSH and GSSG) were distinguished in ^{13}C NMR and their relativity *in vivo* could differ depending on liver condition [36], the levels of GSH and GSSG were not separately reported in this study. This was because the relative concentrations of GSH and GSSG *ex vivo* may not reflect relative concentrations in the liver *in vivo*. GSH is dominant *in vivo*, but GSH exposure to air causes time-dependent oxidation [37,38]. We also noticed that the lag of NMR acquisition from tissue preparation tended to increase the ratio of GSSG/GSH, suggesting GSH oxidation during sample preparation and storage. In the quantitation of total glutathione, the signal from each amino acid subunit was analyzed focusing on glycine moiety C2, glutamate moiety C4, and cysteine moiety C3, and the results based on different parts of glutathione were consistent. In theory, singlets from all the carbons in glutathione reflect their pool size, but many other carbons, except the several carbons selected in this study, were not suitable for precise analysis. The signals from other carbons in glutathione were hard to discern due to close proximity or overlap with signals from other metabolites. In our previous study with hamsters, the singlet signal from glutamate moiety C4 was quantified to report a glutathione pool size in the liver altered by an acetaminophen overdose [39]. Though [U–$^{13}C_3$] glycerol was injected intraperitoneally to the rodents, liver glutathione was not labeled by ^{13}C. It was not a surprise because the experimental conditions with the hamsters were quite different from the current work. In our understanding, this study is the first report regarding glycerol incorporation to hepatic glutathione in mammals.

The use of [U–$^{13}C_3$]glycerol provided some insight about the biosynthesis of glutathione in the liver of obese young volunteers though it should be taken with caution because the duration from the glycerol administration to liver biopsy varied among patients. Nevertheless, the trends of impaired glutathione synthesis was obvious in the presence of steatosis or inflammation, and the newly synthesized glutathione through glutamate was significantly decreased in the fibrotic liver. There were controversial reports about hepatic glutathione contents in rodent models of hepatic steatosis. A choline deprived diet initially increased liver glutathione up to 3 days but decreased it afterward [40] while mitochondrial glutathione was reported to increase in the fatty liver of ob/ob mice [41]. It has been proposed that glutathione is consumed as a compensatory protection against further hepatic pathology. This idea is supported by several recent clinical investigations of glutathione for treatment of NAFLD. Specifically, previous reports have shown that four months of 300 mg/day of glutathione treatment improves ALT and lipid profiles in NAFLD patients [36] and decreases oxidative stress measured by serum 8-hydroxy-2-deoxyguanosine in a second cohort of individuals with NASH [42]. Taken together with our data, this suggests that the demand and utilization of glutathione is closely related with liver pathophysiology. Given that our study included young volunteers with normal to mild liver pathology, we cannot make any definitive conclusions about how glutathione metabolism may differ across the NAFLD spectrum. Therefore, future work with larger sample sizes should investigate the interactions among glutathione synthesis, utilization, and detoxification in individuals with advanced or chronic fatty liver disease and further, explore how these processes may relate to disease progression.

6. Conclusions

This study demonstrates glycerol incorporation into glutathione through glycine and glutamate metabolism in human liver. Glycerol, a substrate traditionally associated with gluconeogenesis, was utilized for glutathione synthesis. Since the majority of participants studied had little evidence of significant liver disease, the roles of glycerol in liver pathophysiology require further investigation in larger sample sizes and individuals across the entire spectrum of fatty liver disease. It would be interesting to investigate whether glycerol incorporation into glutathione is related to fatty liver disease progression. Further work should also investigate the partitioning of glycerol for gluconeogenesis, fatty acid esterification, or glutathione synthesis in relation to other chronic liver diseases.

Funding

This study was supported by the National Institutes of Health [EB015908; DK058398; multi-center nutrition and obesity center pilot from P30DK056336; NIH/NCATS Colorado CTSA Grant Number UL1 TR002535] and the Childrens Hospital Colorado Department of Pediatric Surgery.

Author declarations

1. Eunsook S. Jin: Conceptualization; Data curation; Formal analysis; Methodology; Roles/Writing - original draft;
2. Craig R. Malloy: Conceptualization; Data curation; Formal analysis; Methodology; Validation; Visualization; Roles/Writing - original draft;
3. Gaurav Sharma: Data curation; Formal analysis; Methodology; Validation; Visualization; Writing - review & editing.
4. Erin Finn Data curation; Formal analysis; Investigation; Roles/Writing - original draft;
5. Kelly N. Z. Fuller Data curation; Formal analysis; Investigation; Roles/Writing - original draft;
6. Yesenia Garcia Reyes Data curation; Investigation; Methodology; Project administration; Supervision; Writing - review & editing.
7. Mark A. Lovell Data curation; Investigation; Writing - review & editing.
8. Sarkis C. Derderian Data curation; Investigation; Writing - review & editing.
9. Jonathan A. Schoen Data curation; Investigation; Writing - review & editing.
10. Thomas H. Inge Conceptualization; Data curation; Funding acquisition; Investigation; Supervision; Writing - review & editing.
11. Melanie G. Cree Conceptualization; Data curation; Formal analysis; Funding acquisition; Investigation; Methodology; Project administration; Supervision; Validation; Visualization; Roles/Writing - original draft; .

Declaration of competing interest

None.

Data availability

Data will be made available on request.

Acknowledgements

The authors would like to thank the patients and their family members for participating, and the Children's Hospital Colorado operating room staff for their assistance in performing the research.

Appendix A. Supplementary data

Supplementary data to this article can be found online at https://doi.org/10.1016/j.redox.2023.102749.

References

[1] J.B. Schwimmer, et al., Prevalence of fatty liver in children and adolescents, Pediatrics 118 (4) (2006) 1388–1393.
[2] E.L. Anderson, et al., The prevalence of non-alcoholic fatty liver disease in children and adolescents: a systematic review and meta-analysis, PLoS One 10 (10) (2015), e0140908.
[3] N. Alkhouri, et al., Liver transplantation for nonalcoholic steatohepatitis in young patients, Transpl. Int. 29 (4) (2016) 418–424.
[4] S.A. Xanthakos, et al., Progression of fatty liver disease in children receiving standard of care lifestyle advice, Gastroenterology 159 (5) (2020) 1731–1751 e10.
[5] C. Mandato, et al., Metabolic, hormonal, oxidative, and inflammatory factors in pediatric obesity-related liver disease, J. Pediatr. 147 (1) (2005) 62–66.
[6] V. Ribas, C. Garcia-Ruiz, J.C. Fernandez-Checa, Glutathione and mitochondria, Front. Pharmacol. 5 (2014) 151.
[7] J. Pizzorno, Glutathione!, Integr. Med. 13 (1) (2014) 8–12.
[8] G. Wu, et al., Glutathione metabolism and its implications for health, J. Nutr. 134 (3) (2004) 489–492.
[9] A. Pastore, et al., Determination of blood total, reduced, and oxidized glutathione in pediatric subjects, Clin. Chem. 47 (8) (2001) 1467–1469.
[10] S.C. Lu, Glutathione synthesis, Biochim. Biophys. Acta 1830 (5) (2013) 3143–3153.
[11] K.M. Halprin, A. Ohkawara, The measurement of glutathione in human epidermis using glutathione reductase, J. Invest. Dermatol. 48 (2) (1967) 149–152.
[12] M. Kretzschmar, Regulation of hepatic glutathione metabolism and its role in hepatotoxicity, Exp. Toxicol. Pathol. 48 (5) (1996) 439–446.
[13] P. E, J.J. K, Glutathione: physiological and clinical relevance, Journal of Restorative Medicine 1 (1) (2012).
[14] M. Ookhtens, N. Kaplowitz, Role of the liver in interorgan homeostasis of glutathione and cyst(e)ine, Semin. Liver Dis. 18 (4) (1998) 313–329.
[15] S.C. Lu, Regulation of glutathione synthesis, Mol. Aspect. Med. 30 (1–2) (2009) 42–59.
[16] P.I. Moreira, et al., Lipoic acid and N-acetyl cysteine decrease mitochondrial-related oxidative stress in Alzheimer disease patient fibroblasts, J Alzheimers Dis 12 (2) (2007) 195–206.
[17] W.M. Lee, Acetaminophen and the U.S. Acute liver failure study group: lowering the risks of hepatic failure, Hepatology 40 (1) (2004) 6–9.
[18] W.M. Lee, et al., Acute liver failure: summary of a workshop, Hepatology 47 (4) (2008) 1401–1415.
[19] C. Persaud, T. Forrester, A.A. Jackson, Urinary excretion of 5-L-oxoproline (pyroglutamic acid) is increased during recovery from severe childhood malnutrition and responds to supplemental glycine, J. Nutr. 126 (11) (1996) 2823–2830.
[20] R.F. Grimble, et al., Cysteine and glycine supplementation modulate the metabolic response to tumor necrosis factor alpha in rats fed a low protein diet, J. Nutr. 122 (11) (1992) 2066–2073.
[21] G.M. Mabrouk, M. Jois, J.T. Brosnan, Cell signalling and the hormonal stimulation of the hepatic glycine cleavage enzyme system by glucagon, Biochem. J. 330 (Pt 2) (1998) 759–763.
[22] A. Mardinoglu, et al., Personal model-assisted identification of NAD(+) and glutathione metabolism as intervention target in NAFLD, Mol. Syst. Biol. 13 (3) (2017) 916.
[23] O. Rom, et al., Glycine-based treatment ameliorates NAFLD by modulating fatty acid oxidation, glutathione synthesis, and the gut microbiome, Sci. Transl. Med. 12 (572) (2020).
[24] R.V. Sekhar, et al., Glutathione synthesis is diminished in patients with uncontrolled diabetes and restored by dietary supplementation with cysteine and glycine, Diabetes Care 34 (1) (2011) 162–167.
[25] J.L. Mauriz, et al., Dietary glycine inhibits activation of nuclear factor kappa B and prevents liver injury in hemorrhagic shock in the rat, Free Radic. Biol. Med. 31 (10) (2001) 1236–1244.
[26] K.A. Cieslik, et al., Improved cardiovascular function in old mice after N-acetyl cysteine and Glycine supplemented diet: inflammation and mitochondrial factors, J Gerontol A Biol Sci Med Sci 73 (9) (2018) 1167–1177.
[27] D. Nguyen, et al., Effect of increasing glutathione with cysteine and glycine supplementation on mitochondrial fuel oxidation, insulin sensitivity, and body composition in older HIV-infected patients, J. Clin. Endocrinol. Metab. 99 (1) (2014) 169–177.
[28] A. Ruiz-Ramirez, et al., Glycine restores glutathione and protects against oxidative stress in vascular tissue from sucrose-fed rats, Clin. Sci. (Lond.) 126 (1) (2014) 19–29.
[29] E.S. Jin, A.D. Sherry, C.R. Malloy, An oral load of [13C3]Glycerol and blood NMR analysis detect fatty acid esterification, pentose phosphate pathway, and glycerol metabolism through the tricarboxylic acid cycle in human liver, J. Biol. Chem. 291 (36) (2016) 19031–19041.
[30] D.E. Kleiner, et al., Design and validation of a histological scoring system for nonalcoholic fatty liver disease, Hepatology 41 (6) (2005) 1313–1321.
[31] O. Fiehn, Metabolomics by gas chromatography-mass spectrometry: combined targeted and untargeted profiling, Curr. Protoc. Mol. Biol. 114 (2016) 30 4 1–30 4 32.
[32] R. Pelkonen, E.A. Nikkila, M. Kekki, Metabolism of glycerol in diabetes mellitus, Diabetologia 3 (1) (1967) 1–8.
[33] I. Puhakainen, V.A. Koivisto, H. Yki-Jarvinen, Lipolysis and gluconeogenesis from glycerol are increased in patients with noninsulin-dependent diabetes mellitus, J. Clin. Endocrinol. Metab. 75 (3) (1992) 789–794.
[34] A. Fu, et al., Glucose metabolism and pyruvate carboxylase enhance glutathione synthesis and restrict oxidative stress in pancreatic islets, Cell Rep. 37 (8) (2021), 110037.
[35] M. Suzuki, et al., Substrates for glutathione regeneration in mammalian erythrocytes, Comparative Haematology International 7 (1997) 70–73.
[36] Y. Honda, et al., Efficacy of glutathione for the treatment of nonalcoholic fatty liver disease: an open-label, single-arm, multicenter, pilot study, BMC Gastroenterol. 17 (1) (2017) 96.
[37] T. Tomin, M. Schittmayer, R. Birner-Gruenberger, Addressing glutathione redox status in clinical samples by two-step alkylation with N-ethylmaleimide isotopologues, Metabolites 10 (2) (2020).
[38] D.M. Townsend, K.D. Tew, H. Tapiero, The importance of glutathione in human disease, Biomed. Pharmacother. 57 (3–4) (2003) 145–155.
[39] E.S. Jin, M.H. Lee, C.R. Malloy, Divergent effects of glutathione depletion on isocitrate dehydrogenase 1 and the pentose phosphate pathway in hamster liver, Phys. Rep. 8 (16) (2020), e14554.
[40] I. Grattagliano, et al., Severe liver steatosis correlates with nitrosative and oxidative stress in rats, Eur. J. Clin. Invest. 38 (7) (2008) 523–530.
[41] S. Yang, et al., Mitochondrial adaptations to obesity-related oxidant stress, Arch. Biochem. Biophys. 378 (2) (2000) 259–268.
[42] M. Irie, et al., Reduced glutathione suppresses oxidative stress in nonalcoholic fatty liver disease, Euroasian J. Hepato-Gastroenterol. 6 (1) (2016) 13–18.